The Journal of Chemical Physics ARTICLE scitation.org/journal/jcp

Pulse-shaped chopping: Eliminating and characterizing heat effects in ultrafast infrared spectroscopy

Cite as: J. Chem. Phys. 153, 204201 (2020); doi: 10.1063/5.0031581
Submitted: 1 October 2020 • Accepted: 6 November 2020 •
Published Online: 24 November 2020

David J. Hoffman, Sebastian M. Fica-Contreras, Junkun Pan, and Michael D. Fayer[a)]

AFFILIATIONS

Department of Chemistry, Stanford University, Stanford, California 94305, USA

[a)]Author to whom correspondence should be addressed: fayer@stanford.edu. Telephone: 650 723-4446

ABSTRACT

The infrared pulses used to generate nonlinear signals from a vibrational probe can cause heating via solvent absorption. Solvent absorption followed by rapid vibrational relaxation produces unwanted heat signals by creating spectral shifts of the solvent and probe absorptions. The signals are often isolated by "chopping," i.e., alternately blocking one of the incident pulses. This method is standard in pump–probe transient absorption experiments. As less heat is deposited into the sample when an incident pulse is blocked, the heat-induced spectral shifts give rise to artificial signals. Here, we demonstrate a new method that eliminates heat induced signals using pulse shaping to control pulse spectra. This method is useful if the absorption spectrum of the vibrational probe is narrow compared to the laser bandwidth. By using a pulse shaper to selectively eliminate only frequencies of light resonant with the probe absorption during the "off" shot, part of the pulse energy, and the resulting heat, is delivered to the solvent without generating the nonlinear signal. This partial heating reduces the difference heat signal between the on and off shots. The remaining solvent heat signal can be eliminated by reducing the wings of the on shot spectrum while still resonantly exciting the probe; the heat deposition from the on shot can be matched with that from the off shot, eliminating the solvent heat contribution to the signal. Modification of the pulse sequence makes it possible to measure only the heat signal, permitting the kinetics of heating to be studied.

I. INTRODUCTION

Ultrafast infrared (IR) nonlinear spectroscopy is a powerful technique used for elucidating structural and dynamical information from a wide variety of physical and chemical systems.[1–7] In general, nonlinear spectroscopy involves the interaction of a sample with multiple pulses of light at variable times to generate the desired signal. The nonlinear signal is typically isolated from its background or unwanted scattered light in one of two ways: either through a "phase-cycling" strategy,[8–10] where the sign of the nonlinear signal is inverted by shifting the phase of one or more of the interacting pulses, which then facilitates the elimination of background and scattered light by subtracting the various signals from each other. The alternative is the "chopping" strategy,[9–11] in which one of the pulses is alternately blocked and unblocked with a mechanical chopper or an acousto-optic modulator (AOM), causing the nonlinear signal to also turn on and off. As in the phase cycling strategy, the background is then eliminated by subtracting the measured "off" signal from the "on" signal. The chopping technique is necessary for signals that are not dependent on the relative phases of the interacting pulses, such as in a transient absorption (pump–probe) experiment.[8,10]

However, each of the individual pulses of light will also be partially absorbed by both the vibrational probe of interest and various solvent modes. The solvent modes generally deposit heat by vibrational relaxation on very fast time scales into the system.[5,12–16] The heat profile will diffuse on slow time scales (microseconds or longer), depending on the transport thermal characteristics of the chemical system.[17] This solvent heating can change the absorption spectrum of the chromophore.[12] When the chopping method is used to obtain a nonlinear signal, it also blocks one of the pulses that would be partially absorbed by the sample. The change in the amount of

light between the on and off shots results in a different heat profile in the sample between the two shots. The differing amounts of heat can cause an unwanted difference signal from heat-induced changes to the chromophore's or solvent's absorption in addition to the desired resonant signal from the probe. As the signal from linear absorption is typically many orders of magnitude larger than a third order nonlinear signal,[2] a minuscule change in the absorption spectrum can result in a differential heat signal on the same scale as the desired nonlinear signal. The heating signal then needs to be modeled and subtracted to obtain the desired nonlinear signal.[5] These heat signals tend to be isotropic (no polarization dependence) even before complete thermalization, which simplifies these analyses, but anisotropic effects have been seen in some chemical systems.[18]

To address the problem of unwanted heat signals, we have employed a germanium AOM functioning as a pulse shaper. Pulse shaping has already been widely used in nonlinear spectroscopy, as it enables the collection of 2D spectra in a pump–probe geometry,[8] data collection and scatter suppression through phase cycling,[8,19,20] and collection of 2D interferograms in a rotating frame.[8,21] In addition, it has been shown that by using a pulse shaper to selectively block a range of frequencies in a pulse spectrum, the effects of coherent oscillations or population transfer between coupled vibrational modes can be suppressed.[19,22,23] This last technique demonstrates the ability of pulse shapers to selectively block the excitation of a chromophore mode while delivering the rest of the energy of the pulse to the desired mode. A modification of this method is the basis of this work.

II. METHOD AND RESULTS

The experiments were conducted on the CN stretch of phenylselenocyanate (PhSeCN) in dimethylformamide (DMF). The CN stretch of PhSeCN has a very long lifetime, 225 ps–430 ps,[15,24] depending on the solvent environment, which makes it a useful probe for systems that have both fast and slow dynamics. However, it has small transition dipole, which results in weak nonlinear signals, making it sensitive to even a small amount of heating signal. Figure 1 is a background subtracted spectrum of the CN stretch. The peak is at 2152 cm^{-1} and the full width at half maximum (FWHM) linewidth is 10.25 cm^{-1}. For the application of the suppression of the heat signal method to work, the pulse bandwidth must be large compared to the width of the absorption of interest. The IR pulses have a FWHM bandwidth of 100 cm^{-1}, which meets the condition. Figure 2(a) shows the full transmittance spectrum (black curve) without background subtraction. There is substantial solvent absorption within the IR pulse bandwidth. Therefore, in addition to the excitation of the CN stretch, the solvent absorbs a significant amount of IR. The solvent absorption, which is a lumpy continuum, is likely a combination of intramolecular overtones and combination bands of DMF as well as combinations of intramolecular modes with intermolecular solvent modes. Such vibrational excitations tend to have short lifetimes, resulting in rapid deposition of heat into the solvent.[17,25–28]

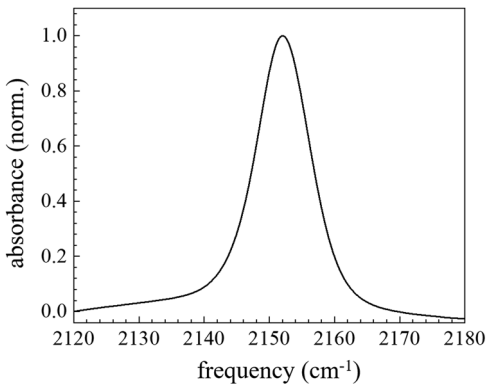

FIG. 1. The background subtracted absorption spectrum of the CN stretch of phenylselenocyanate (PhSeCN) in dimethylformamide (DMF).

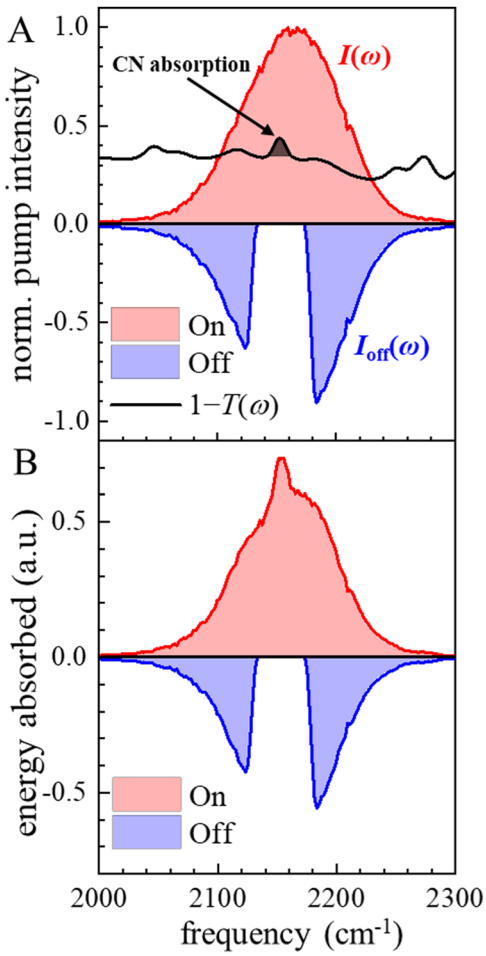

FIG. 2. (a) Filled red curve: the unmodified pump pulse spectrum (on pulse). Filled blue curve: spectrum with the frequency hole so that the CN stretch is not excited (off pulse). The off pulse is negative-going to indicate the subtraction of signals in the modulation scheme. Black curve: one minus the transmission spectrum of the DMF background absorption and the CN stretch absorption (filled black peak) centered at 2152 cm^{-1}. (b) The same as (a) but showing the energy absorbed by the on and off pulses rather than their spectra.

The method of selectively blocking frequencies was employed to create a modified modulation (chopping) scheme using an AOM pulse shaper. Instead of using the AOM or mechanical chopper to block the entire pump pulse for the "off" shot, the pulse spectrum was modified to eliminate frequencies corresponding to the chromophore absorption. These data were subtracted from the on shot. Therefore, the on shot excites the chromophore and the off shot does not. This stratagem acts like chopping, but part of the solvent spectrum is still excited by the modified "off" pulse.

An illustration is shown in Fig. 2(a), where the filled blue curve (flipped upside down, indicating the subtraction) is the modified spectrum with the frequencies resonant with the vibrational probe (black curve, peak at 2152 cm^{-1}) selectively blocked. This serves the same purpose as the original chopping scheme of switching the nonlinear signal off, but it also delivers the remaining energy of the pulse to the solvent. For a given system, neglecting reflectance, the energy delivered at each frequency for a given pulse power spectrum $I(\omega)$ can be determined from

$$E(\omega) = I(\omega)(1 - T(\omega)), \tag{1}$$

where $T(\omega)$ is the transmission spectrum of the system. The fraction of the total energy delivered to the solvent for a given modified off pulse spectrum is obtained by integrating over all frequencies

$$f_{\mathrm{mod}} = \frac{\int E_{\mathrm{mod}}(\omega)d\omega}{\int E(\omega)d\omega} = \frac{\int I_{\mathrm{mod}}(\omega)(1 - T(\omega))d\omega}{\int I(\omega)(1 - T(\omega))d\omega}, \tag{2}$$

where $I(\omega)$ is the unmodified pulse spectrum and $I_{\mathrm{mod}}(\omega)$ is the modified off pulse spectrum. $I(\omega)$ (without subscripts) will refer to an unmodified pulse spectrum throughout this work. Provided there is a linear relationship between energy absorbed, local temperature change, and the difference signal magnitude,[12] which is the most likely situation, the total remaining difference heat signal using the pulse-shaped "chopping" scheme will be reduced by a factor of $1 - f_{\mathrm{mod}}$ relative to the standard chopping procedure. The fraction f_{mod} can be visualized by comparing the area of $E(\omega)$ for the unmodified (red curve) and modified (blue curve) pulses in Fig. 2(b). This new procedure results in a partial suppression of the heating component of the difference signal without any modification to the nonlinear signal or reduction in duty cycle compared to the conventional chopping method.

Another important feature of using the AOM to collect pump–probe data is the ability to suppress scattered light from the pump pulse, which is heterodyned with the probe pulse through phase cycling. As discussed above, the pump–probe signal is not dependent on the relative phase of the pump and probe pulse, and the heat difference signal is also independent of the phase. Therefore, the standard phase cycling scheme for suppressing scatter in the pump–probe experiment can be used with the new modulation scheme. The on and off pulse data are first acquired with one phase of the pump pulse and are then they are acquired with a π phase shift relative to the first pair. Adding the pairs of shots together will suppress phase-dependent scattered light while conserving the phase-independent resonant signal.

From Eq. (2), it can be seen that this method gives the best results when the absorption spectrum is much smaller than the laser bandwidth, such that the difference between the modified pulse intensity spectrum $I_{\mathrm{mod}}(\omega)$ and the initial intensity spectrum $I(\omega)$ is as small as possible. As many important classes of vibrational probes, e.g., nitriles and carbonyls, typically have linewidths of 20 cm^{-1} or less, and ultrafast IR spectroscopy regularly uses femtosecond light sources, this condition is often met.

Depending on the system and the required level of heat suppression, the approach depicted in Fig. 2 can be extended by modifying the "on" shot pulse spectrum as well. In practice, when the energy fraction f_{mod} can be matched for the on (f_{on}) and off (f_{off}) shots, then the heating effects on the desired data can be completely suppressed. The on shot can be modified in two ways. The first is through selective elimination of pulse frequencies that do not excite the vibrational chromophore. This approach is illustrated by the filled red curve in Fig. 3(a). If $f_{\mathrm{off}} > 0.5$, then the heat signal in principle can be completely removed with no reduction in the nonlinear signal intensity. $f_{\mathrm{off}} > 0.5$ is essentially the condition that the pulse bandwidth is large compared to the absorption spectrum of the vibrational probe under study, and the solvent has non-negligible absorption throughout the pulse bandwidth. By reducing the wings of the on shot spectrum to match f_{on} and f_{off}, the pulse duration will be increased, which will reduce the time resolution of the nonlinear experiment. However, the fastest measurable dynamics are the inverse of the width of the absorption spectrum.[2] Therefore, the reduction in time resolution should not be a problem because the on pulse reduced bandwidth is larger than the absorption bandwidth. An illustration of the energy deposited with f_{on} and f_{off} matched is shown in Fig. 3(b).

In the second method, a uniform reduction in the intensity of the on pulse by a factor of $f_{\mathrm{off}}/f_{\mathrm{on}}$ would be used. This approach works for arbitrary $f_{\mathrm{off}} > 0$ and does not affect the pulse duration. However, if f_{off} is small, there will be a large reduction in the on pulse energy, and the signal will be reduced significantly.

To illustrate the new method for the elimination of heating on the nonlinear signal illustrated in Figs. 2 and 3, the pulse-shaping chopping scheme was applied to IR polarization-selective pump–probe experiments on the CN stretch of PhSeCN in DMF, a system with a strong background absorption. As mentioned above, the CN stretch of PhSeCN has a long vibrational lifetime but a small transition dipole. Therefore, it produces weak nonlinear signals. The ultrafast IR equipment employed here has been described in detail in prior work.[15,21,29] 800 nm pulses from a Ti:Sapphire oscillator/regen pumped a home-built optical parametric amplifier (OPA) to generate mid-IR pulses at 4.6 μm with a 100 cm^{-1} FWHM. This 100 cm^{-1} bandwidth is much broader than the ~10 cm^{-1} absorption spectrum of the CN stretch of PhSeCN (see Figs. 2 and 3). Each mid-IR pulse is split into a strong pump pulse, which passes through the AOM pulse shaper and a weaker probe pulse, which travels down a mechanical delay stage that controls the time delay between the pump and probe pulses. The two pulses are spatially overlapped in the sample. Prior to the sample, the pump pulse passes through a half wave plate and polarizer set to +45° relative to the probe pulse. After the sample, the probe is alternately resolved at ±45° every other delay line scan to determine the signals

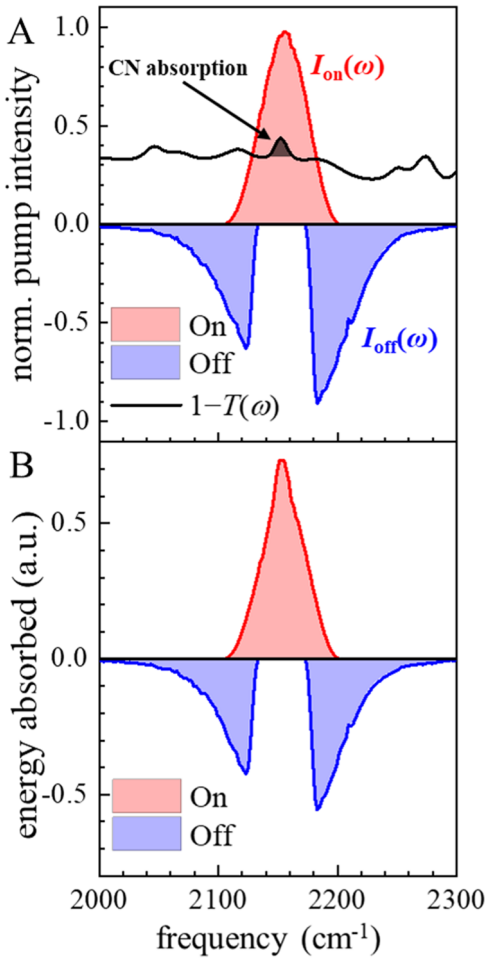

FIG. 3. (a) Equivalent of Fig. 2(a) but now the pump spectrum (filled red curve) has been reduced in width so that it still excites the CN stretch (filled black peak) but the energy delivered to the solvent by the pump (on pulse) is the same as the energy delivered by the off pulse (blue spectrum). (b) The same as (a) but showing the energy absorbed by the on and off pulses rather than their spectra. It was found that for a complete elimination of the heat signature in this system, the energy delivered by the on pulse had to be less than that of the off pulse (f_{on} = 0.44, f_{off} = 0.52).

polarized parallel and perpendicular relative to the pump pulse. The isotropic signal is constructed from a linear combination of the parallel and perpendicular signals ($I_{\parallel} + 2I_{\parallel}$), which is equivalent to the signal obtained at the magic angle.[6,7] This signal is the vibrational population relaxation, which should be a single exponential decay.

Four different pulse-shaping modulations schemes were applied to the PhSeCN/DMF system to illustrate the utility and effectiveness of the method. The decay of the isotropic pump–probe signal from the CN stretch should be a single exponential decay. Data were collected for >1.5 ns, which is made possible by the very long CN stretch lifetime of PhSeCN. First, applying the standard chopping sequence [On: $I(\omega)$, Off: 0], the isotropic signal of PhSeCN in DMF has a large heat induced artifact at long waiting times. This offset is clearly seen in the black curve in Fig. 4(a), where the isotropic signal is highly non-exponential and goes to a constant value of ~10% of the initial signal at a very long time. The blue points [on: $I(\omega)$; off: $I_{off}(\omega)$; see Fig. 2] are closer to exponential. $I_{off}(\omega)$ deposits a reduced amount of heat but it is still less than $I(\omega)$ resulting in a smaller heat induced signal. The net difference in the amount of heat deposited by this approach is reduced but not eliminated because $I_{off}(\omega)$ does not excite the solvent spectral range in the frequency hole around the CN stretch. The red points are for the full modulation method [on: $I_{on}(\omega)$; off: $I_{off}(\omega)$; see Fig. 3]. With these pulse-shaped pulses, the amount of heat deposited by the on pulse and the off pulse was made to be the same. Their difference eliminates the heat signal while generating the desired resonant isotropic signal. As can be seen in Fig. 4(a), the decay is a single exponential.

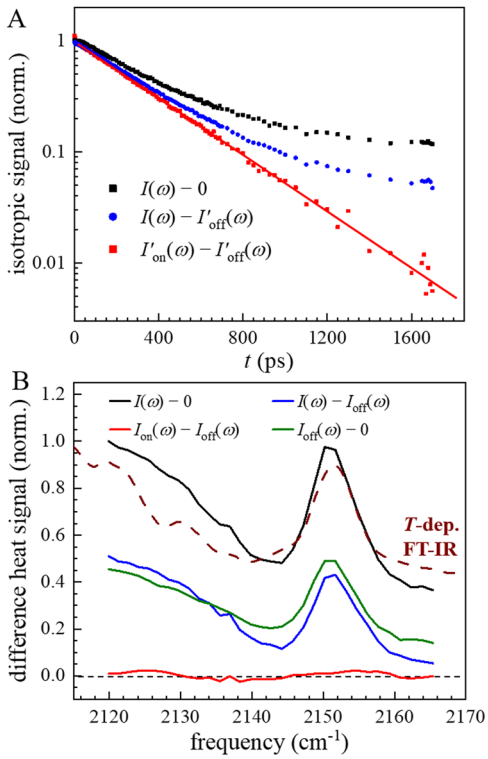

FIG. 4. (a) Isotropic signals of the CN stretch of PhSeCN in DMF at the center frequency of the CN absorption (2152 cm^{-1}) for the three chopping schemes discussed in the main text. The black points are the standard on/off chopping signal. There is a large heat signal giving a non-exponential decay to a large off-set. The blue points are for the on/off pulses shown in Fig. 2(a). The heat artifact is reduced. The red points show the results of the full heat suppression method illustrated in Fig. 3(a). The signal is now a single exponential decay with no heat induced signal artifacts. (b) Spectra of the long time heat signal for the three chopping schemes and the inverted chopping scheme discussed in the main text. The full heat suppression method (red curve) shows no heat signal within experimental noise. The wine colored dashed curve represents the heat signature calculated from temperature dependent FT-IR experiments and corresponds to a 0.3 K temperature increase.

The isotropic nonlinear signal should decay exponentially to zero with the lifetime of the CN stretch (~340 ps in DMF). By fitting the isotropic decays using the standard chopping sequence, $I(\omega) - 0$, at all frequencies as single exponentials to an offset, the spectrum of the asymptotic heat signal can be determined by the amplitude of the offset [Fig. 4(b), black curve]. It should be noted that the decay at short time has a deviation from exponential behavior. This deviation has been shown below to arise from heat effects; so, for extracting the spectra in Fig. 4(b), the fits are begun at 15 ps to avoid the nonexponential behavior. The black curve shows two main features. There is the very broad somewhat structured continuum and the peak that arises from the CN stretch at 2152 cm^{-1} [see the black curve in Fig. 2(a)]. The deposition of heat causes the heat signal spectrum by producing very small shifts in the positions and amplitudes of the absorptions. These spectral shifts cause the signal with the pump on and the pump off to differ because of the different amounts of deposited heat. Therefore, the difference between on and off gives a heat signal in addition to the nonlinear signal generated by the CN stretch.

Absorption by the solvent is followed by rapid vibrational relaxation, which results in a temperature jump, mainly through the excitation of low frequency intermolecular modes.[17,25–28] There are two sources of the heat signal, density change and temperature change. Following the rapid radiationless relaxation of the solvent vibrational excitations, the solvent temperature has increased while the density has remained unchanged. The final temperature jump was calculated to be ~0.5 K using the 10 μJ pump pulse energy, the excitation volume (~2 × 10^6 μm^3), and the DMF heat capacity, 146 J/(K mol), and found to be in reasonable agreement with temperature dependent Fourier transform infrared (FT-IR) measurements. The heat signature was calculated from a combination of temperature dependent FT-IR spectra of the PhSeCN/DMF system and the pulse spectrum in Fig. 2(a). The results are shown in Fig. 4(b) (dashed wine colored curve) and is based on a temperature change of 0.3 K. The initial T-jump itself can induce a heat signal. The temperature jump will, for example, cause increased excitations of librational modes. Because the potentials are anharmonic, the increase in librational excitations results in a shift of the equilibrium configurations. Such very small changes in the liquid structure modify solvent–solvent and solvent–probe intermolecular interactions, resulting in frequency shifts. These shifts will occur for the on shot but not for the off shot with standard chopping, giving rise to a heat signal. The T-jump frequency shifts will occur very rapidly but not instantaneously. Vibrational relaxation and thermalization can occur on sub-ps to many ps time scales. There can even be a delay between the relaxation of the initially excited vibrations and an increase in the temperature, which requires thermalization among all modes. The delay can be caused by the initial relaxation into lower frequency intramolecular modes and their subsequent relaxation into all solvent degrees of freedom.[13]

The T-jump launches an acoustic wave that propagates radially outward from the excited laser spot. The density change occurs with the time required for the acoustic wave to travel the diameter of the laser spot size. For a typical diameter of 200 μm and a typical velocity of sound of 2 × 10^3 m/s, the time is ~10 μs.[17] This time is long compared to the time scale of the experiment (~1 ns). However, once the density has changed, it decays to normal density with the rate of thermal diffusion, which is slow.[17] The thermal diffusivity of DMF at room temperature[30] is slightly less than 10 mm^2/s and the pump beam spot size is ~100 μm, giving a thermal relaxation time of ~1 ms.[17] Therefore, following the on shot, the density change is present at the time of the off shot unless the laser spot size is very small and the repetition rate is very low. If the off shot deposits no heat, the density change continues to decay to a lower level by the next on shot. Therefore, there is a density difference between the off shot and the on shot. The density change signal is likely to be larger than the temperature increase signal.

The second scheme uses the modified pump spectrum with the resonant frequencies selectively blocked for the off shot, but does not change the on shot [on: $I(\omega)$; off: $I_{off}(\omega)$; see Fig. 2]. The heat signal determined from the long term offset of the decay [blue points, Fig. 4(a)] is reduced by slightly more than half [blue curve, Fig. 4(b)], which agrees well with the predicted value from Eq. (2) (f_{off} = 0.52, with residual heat $1 - f_{off}$). Additionally, the non-exponential behavior near time zero is greatly reduced. The remaining heat signal was further suppressed, essentially to zero, by applying the modifications of the on pulse described above (see Fig. 3). As $f_{off} > 0.5$ in this system, the on pulse was modified to block the necessary amount of the non-resonant frequencies [on: $I_{on}(\omega)$; off: $I_{off}(\omega)$] while maintaining an approximately Gaussian profile. The result is the red curve in Fig. 4(b). The dashed black line is set at zero as an aid to the eye. This method was able to reduce the total amplitude to the point where it fluctuates around zero. It should be noted that to achieve the degree of cancellation shown in Fig. 4, the value of f_{on} (0.44) had to be reduced below f_{off} (0.52), indicating that further adjustments beyond the value predicted in Eq. (2) can be necessary for best results. Furthermore, the bandwidth of the pulse was reduced by almost a factor of three [filled red curve in Fig. 3(a)]. However, it is still substantially broader than the CN stretch spectrum. As discussed above, this bandwidth is sufficient to measure all observable dynamics.

The heat signal can be isolated for study by another pulse sequence. In this sequence, the on shot selectively blocks frequencies resonant with the chromophore [see blue spectrum in Fig. 2(a) or 3(a)] and the off shot has zero pulse intensity as in the standard chopping scheme [on: $I_{off}(\omega)$; off: 0]. Therefore, there is no resonant CN excitation on either shot. The green curve in Fig. 4(b) displays a similar asymptotic heat signature as the blue curve, with amplitude f_{off} = 0.52 relative to the normal chopping procedure. These results provide additional validation for the method. However, as there should be no CN stretch signal generated using this cycle, the heat signal can be observed at all times, including at early times where the magnitude of the heat signal is usually much smaller than a probe's resonant nonlinear signal. This pulse sequence gives access to the time-dependent heat kinetics of a system while also enabling rigorous quantification of the magnitude of the heat signal.

The time and polarization dependence of the heat signals for the CN stretch of PhSeCN in DMF using the inverted procedure is shown in Fig. 5. There are two main time scales visible. First, a fast growth appears with a time constant of 11.8 ± 0.4 ps, which is a result of the relaxation of the initial DMF vibrational excitations and subsequent thermalization of the relaxed vibrations among all of the low frequency modes of the liquid. The fast rise has the

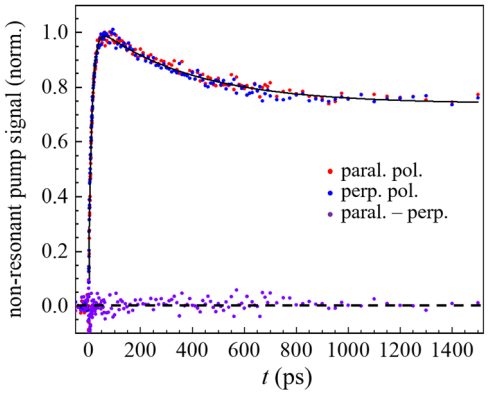

FIG. 5. The parallel and perpendicular polarization signals and their difference using the inverted chopping scheme that eliminates the direct resonant excitation of the CN stretch of the vibrational probe. The rising edge is the growth of the heat signal with an 11.8 ps time constant. All of the data are polarization independent. After the fast rise, there is a 340 ps decay to the long time heat signal. The 340 ps decay is the lifetime of the CN stretch, which is not directly excited. A Raman scattering mechanism that produces Stokes and anti-Stokes photons at the CN absorption frequency is proposed to explain the 340 ps decay feature.

same spectrum as the green curve in Fig. 4(b). The fast growth is responsible for the early nonexponential behavior that is visible in the isotropic signal with the standard chopping cycle [black points, Fig. 4(a)]. Following the fast growth, the signal decays with a time constant of 337 ± 4 ps to a large offset, the offset being the long lived heat signal shown in Fig. 3(b) (black points). The 340 ps decay is the lifetime of the CN stretch. It would be anticipated that the fast rise resulting from DMF vibrational relaxation and heat thermalization would go directly to a very long-lived plateau, that is, after the rise, the data would be horizontal on the time scale of the measurement and much longer. As can be seen in Fig. 5, the entire signal is isotropic. Within error, the parallel and perpendicular polarizations are the same even at short times as shown by their difference (the purple points in Fig. 5). When the CN stretch is excited resonantly with a pump pulse that does not have a spectral hole at the CN stretch absorption frequencies, the parallel and perpendicular polarization signals show the expected large differences at short times compared to the PhSeCN orientational relaxation. At short times, the resonantly excited parallel signal is approximately three times larger than the perpendicular signal. In addition, the parallel signal decays rapidly while the perpendicular signal grows in because of the PhSeCN orientational relaxation. The fact that the 340 ps decay in the heat signal shows no polarization dependence demonstrates that the CN stretch is not being directly excited by AOM "leakage" of light in the frequency range within the hole.

Pump–probe experiments examining the frequency range of the CN stretching mode show the characteristic positive-going 0–1 vibrational transition and the negative-going 1–2 vibrational transition. This spectrum is observed as early as 500 fs, the shortest time accessible. The heat signal grows in with a time constant of ~12 ps and does not reach its peak for ~60 ps. Therefore, the slowly decaying signal is not related to the deposition of heat.

Radiationless excitation via the transfer of energy from an excited DMF molecule to the CN stretch of PhSeCN can also be ruled out. When a DMF molecule absorbs a photon from the pump pulse with the frequency hole in it [see Fig. 2(a)], the excited vibration or combination of vibrations has energy either slightly lower or slightly higher than the CN stretch frequency. The differences in energy between the DMF excitations and the CN stretch are in the range of a few to a few tens of wavenumbers. If an excited DMF is adjacent to the CN, a lower frequency DMF intramolecular vibration(s) plus a mode of the intermolecular continuum can transfer energy and excite the CN vibration. Referring to the intermolecular continuum modes as phonons, the DMF vibrational state and the phonon are annihilated and a CN vibration is created. If the DMF vibrational state is higher in energy than the CN vibration, then the DMF vibrational state is annihilated and a phonon plus the CN vibration are created.[27] In either case, the energy is conserved. However, this is the reverse of pathways involved in the CN stretch vibrational relaxation. The CN relation time is 340 ps. By detailed balance, populating the CN stretch from an adjacent vibrationally excited DMF cannot be faster than 340 ps. In fact, populating the CN stretch from a vibrationally excited DMF would likely be slower than 340 ps as it would not include the equivalent of CN relaxation pathways that involved intramolecular PhSeCN modes.

A possible mechanism that can explain the basically $t = 0$ excitation of the CN stretch and its subsequent decay without a polarization dependence is Raman scattering. Raman scattering can involve low frequency modes of the solvent continuum. Modes such as librations are Raman active. For instance, such modes are excited in ultrafast optical Kerr effect experiments, which provide a time domain equivalent of the low frequency Raman spectrum.[31] Here, both Stokes and anti-Stokes scattering can play a role. Stokes scattering will excite a mode of the continuum and produce a lower frequency photon. Anti-Stokes scattering will annihilate a phonon and produce a higher frequency photon. Looking at the blue spectrum in Fig. 2(a), the high frequency side extends from about 2180 cm^{-1} to 2260 cm^{-1}. Stokes scattering will result in the production of lower frequency photons that can fall within the spectrum of the CN stretch. The low frequency side extends from ~2125 cm^{-1} to 2040 cm^{-1}. Anti-Stokes scattering will produce higher frequency photons that can excite the CN stretch.

The DMF intermolecular continuum will extend up to hundreds of wavenumbers. Therefore, for any CN frequency, ν, in the inhomogeneous absorption spectrum, there are a vast number of Stokes and anti-Stokes pathways that can produce photons with frequency ν. For IR frequencies near the hole, a low frequency phonon would be excited or annihilated. For frequencies far from the hole, a higher frequency phonon would be excited or annihilated. In principle, any frequency in the IR pulse can scatter to produce a given CN frequency ν. For any one pathway, the Raman scattering probability may be low, but the probability of exciting a CN stretch frequency ν involves the integral over all Stokes and anti-Stokes pathways that produce photons with frequency ν. In addition to the large number of pathways, the phonon occupation number will enhance the scattering probability. For a 20 cm^{-1} mode of the solvent continuum, the occupation number is ~10. Furthermore, given the random nature of the orientation of the polarizability tensors of the phonons and the presumably low symmetry of these modes, the Raman

scattering would be expected to be depolarized, consistent with the data in Fig. 5.

The heat signal is only a small fraction of the resonant signal, and the proposed CN Raman scattering induced signal (RSIS, Fig. 4) is only a fraction of the heat signal. Therefore, the RSIS does not need to be efficient to produce the observed results. When resonant excitation of the CN occurs during the pump–probe experiments, the RSIS would go unnoticed as it is only ~1% of the resonant signal. RSIS has the same lifetime as the resonantly pumped signal, but it would contribute a very small unpolarized component to a polarization dependent experiment. The data presented in Fig. 5 are consistent with the RSIS mechanism. However, the results do not definitively establish RSIS as the mechanism.

III. CONCLUDING REMARKS

The AOM pulse-shaping modulation method is a readily implemented technique that can essentially eliminate heat-induced artifacts in ultrafast infrared experiments that require chopping for data collection. The technique is useful when the vibrational probe's absorption line is narrow compared to the laser pulse spectrum. It is particularly efficacious in chemical systems with substantial background absorption that leads to significant heat induced signals. In the example presented here, we demonstrated the complete elimination of heat induced signals (see Fig. 4).

The full method involves narrowing of the excitation pulse bandwidth, which reduces the time resolution. However, the nature of the method results in the excitation bandwidth being wider than the absorption line of interest. Therefore, sufficient time resolution remains to observe any measurable dynamics. Furthermore, a modification of the method enables the selective elimination of the resonantly pumped nonlinear signal, allowing the dynamics of heat generated signals to be observed. Finally, it was observed that the excitation of the probe CN vibrational mode occurred even though the pump pulse did not contain frequencies resonant with the CN stretch absorption. A Raman scattering mechanism was proposed. Stokes and anti-Stokes scattered photons with frequencies resonant with the CN stretch absorption produced a low amplitude signal, despite the lack of the resonant frequencies in the pump pulse.

ACKNOWLEDGMENTS

This work was supported by the Office of Naval Research by ONR Grant No. N00014-17-1-2656.

DATA AVAILABILITY

The data that support the findings of this study are available from the corresponding author upon reasonable request.

REFERENCES

[1] S. Park, K. Kwak, and M. D. Fayer, Laser Phys. Lett. **4**, 704–718 (2007).
[2] P. Hamm and M. Zanni, *Concepts and Methods of 2D Infrared Spectroscopy* (Cambridge University Press, 2011).
[3] S. Mukamel, *Principles of Nonlinear Optical Spectroscopy* (Oxford University Press, New York, 1995).
[4] M. Cho, G. R. Fleming, and S. Mukamel, J. Chem. Phys. **98**, 5314 (1993).
[5] Y. L. A. Rezus and H. J. Bakker, J. Chem. Phys. **123**, 114502 (2005).
[6] H.-S. Tan, I. R. Piletic, and M. D. Fayer, J. Opt. Soc. Am. B **22**, 2009 (2005).
[7] A. Tokmakoff, J. Chem. Phys. **105**, 1–12 (1996).
[8] S.-H. Shim and M. T. Zanni, Phys. Chem. Chem. Phys. **11**, 748–761 (2009).
[9] Y. Feng, I. Vinogradov, and N.-H. Ge, Opt. Express **25**, 26262 (2017).
[10] R. Bloem, S. Garrett-Roe, H. Strzalka, P. Hamm, and P. Donaldson, Opt. Express **18**, 27067 (2010).
[11] J. Brazard, L. A. Bizimana, and D. B. Turner, Rev. Sci. Instrum. **86**, 053106 (2015).
[12] L. De Marco, J. A. Fournier, M. Thämer, W. Carpenter, and A. Tokmakoff, J. Chem. Phys. **145**, 094501 (2016).
[13] T. Steinel, J. B. Asbury, J. Zheng, and M. D. Fayer, J. Phys. Chem. A **108**, 10957–10964 (2004).
[14] H. Bian, X. Wen, J. Li, and J. Zheng, J. Chem. Phys. **133**, 034505 (2010).
[15] D. J. Hoffman, S. M. Fica-Contreras, and M. D. Fayer, Proc. Natl. Acad. Sci. U. S. A. **117**, 13949–13958 (2020).
[16] K. P. Sokolowsky and M. D. Fayer, J. Phys. Chem. B **117**, 15060–15071 (2013).
[17] H. Graener, R. Zürl, M. Bartel, and G. Seifert, J. Mol. Liq. **84**, 161–168 (2000).
[18] L. Liu, J. Hunger, and H. J. Bakker, J. Phys. Chem. A **115**, 14593–14598 (2011).
[19] J. Nishida, A. Tamimi, H. Fei, S. Pullen, S. Ott, S. M. Cohen, and M. D. Fayer, Proc. Natl. Acad. Sci. U. S. A. **111**, 18442–18447 (2014).
[20] S.-H. Shim, D. B. Strasfeld, Y. L. Ling, and M. T. Zanni, Proc. Natl. Acad. Sci. U. S. A. **104**(36), 14197–14202 (2007).
[21] S. K. Karthick Kumar, A. Tamimi, and M. D. Fayer, J. Chem. Phys. **137**, 184201 (2012).
[22] H. J. B. Marroux and A. J. Orr-Ewing, J. Phys. Chem. B **120**, 4125–4130 (2016).
[23] C. H. Giammanco, P. L. Kramer, S. A. Yamada, J. Nishida, A. Tamimi, and M. D. Fayer, J. Phys. Chem. B **120**, 549–556 (2016).
[24] D. J. Hoffman, S. M. Fica-Contreras, and M. D. Fayer, J. Chem. Phys. **150**, 124507 (2019).
[25] A. Tokmakoff, B. Sauter, and M. D. Fayer, J. Chem. Phys. **100**, 9035 (1994).
[26] A. Tokmakoff, B. Sauter, A. S. Kwok, and M. D. Fayer, Chem. Phys. Lett. **221**, 412–418 (1994).
[27] V. M. Kenkre, A. Tokmakoff, and M. D. Fayer, J. Chem. Phys. **101**, 10618 (1994).
[28] H. Graener, R. Zürl, and M. Hofmann, J. Phys. Chem. B **101**, 1745–1749 (1997).
[29] C. Yan, J. E. Thomaz, Y.-L. Wang, J. Nishida, R. Yuan, J. P. Breen, and M. D. Fayer, J. Am. Chem. Soc. **139**, 16518–16527 (2017).
[30] M. Shokouhi, A. H. Jalili, M. Hosseini-Jenab, and M. Vahidi, J. Mol. Liq. **186**, 142–146 (2013).
[31] N. T. Hunt, A. A. Jaye, and S. R. Meech, Phys. Chem. Chem. Phys. **9**, 2167 (2007).